5-1999

The I-Band Tully-Fisher Relation for Sc Galaxies: 21 Centimeter H I Line Data

Martha P. Haynes
Cornell University

Riccardo Giovanelli
Cornell University

Pierre Chamaraux
Paris Observatory

Luiz N. da Costa
European Southern Observatory

Wolfram Freudling
European Southern Observatory

See next page for additional authors

THE ASTRONOMICAL JOURNAL, 117:2039–2051, 1999 May

THE *I*-BAND TULLY-FISHER RELATION FOR Sc GALAXIES: 21 CENTIMETER H I LINE DATA

MARTHA P. HAYNES AND RICCARDO GIOVANELLI
Center for Radiophysics and Space Research, and National Astronomy and Ionosphere Center,[1] Cornell University, Ithaca, NY 14853

PIERRE CHAMARAUX
Observatoire de Paris, Section de Meudon, Place Jules Janssen, F-92195 Meudon, France; chamarau@mesiob.obspm.fr

LUIZ N. DA COSTA
European Southern Observatory, Karl-Schwarzschild-Strasse 2, D-85748 Garching bei München, Germany; ldacosta@eso.org

WOLFRAM FREUDLING
European Southern Observatory and Space Telescope European Coordinating Facility, Karl-Schwarzschild-Strasse 2, D-85748 Garching bei München, Germany; wfreudli@eso.org

JOHN J. SALZER
Department of Astronomy, Wesleyan University, Middletown, CT 06459; slaz@parcha.astro.wesleyan.edu

AND

GARY WEGNER
Department of Physics and Astronomy, Dartmouth College, Hanover, NH 03755; wegner@kayz.dartmouth.edu
Received 1998 November 30; accepted 1999 January 20

ABSTRACT

A compilation of 21 cm line spectral parameters specifically designed for application of the Tully-Fisher (TF) distance method is presented for 1201 spiral galaxies, primarily field Sc galaxies, for which optical *I*-band photometric imaging is also available. New H I line spectra have been obtained for 881 galaxies. For an additional 320 galaxies, spectra available in a digital archive have been reexamined to allow application of a single algorithm for the derivation of the TF velocity width parameter. A velocity width algorithm is used that provides a robust measurement of rotational velocity and permits an estimate of the error on that width taking into account the effects of instrumental broadening and signal-to-noise. The digital data are used to establish regression relations between measurements of velocity widths using other common prescriptions so that comparable widths can be derived through conversion of values published in the literature. The uniform H I line widths presented here provide the rotational velocity measurement to be used in deriving peculiar velocities via the TF method.

Key words: galaxies: spiral — techniques: spectroscopic

1. INTRODUCTION

One of the most promising global secondary distance indicators is the Tully-Fisher (TF) relation, whereby the distance to a galaxy can be measured from observations of its magnitude and rotation velocity as derived, for example, from the 21 cm line profile (Aaronson & Mould 1986). In recent years, the TF technique has been employed by a number of groups in attempts to map out the peculiar velocity field in the Local Supercluster and beyond. Within the considerable body of work devoted to the application of the TF technique, there remains considerable controversy and disagreement, not only as to the implied characteristics of the local peculiar velocity field but also as to the form of the TF relation itself. Considerable effort has gone into estimating the intrinsic scatter of the relation and correcting for biases that complicate its application (see, e.g., Bottinelli et al. 1986; Teerikorpi 1993; Willick 1994; Federspiel, Sandage, & Tammann 1994; Freudling et al. 1995; Giovanelli et al. 1997c).

To investigate the velocity field in the local universe, we have undertaken a program to measure the peculiar velocities of nearby spiral galaxies via the TF distance method, both field Sbc–Sc galaxies (SFI) and cluster spirals (SCI) (Giovanelli et al. 1996, 1997b, 1997c, 1997d, 1998b, 1998c; Borgani et al. 1997; da Costa et al. 1996, 1998; Freudling et al. 1999). The basic observational ingredients for the application of the TF relation are photometric images, which provide both the magnitude variable and an estimate of the galaxy's inclination, and an indicator of rotational velocity, typically provided either by the radio 21 cm H I emission line or by the optical Hα and/or [N II] emission lines. In previous papers, we have discussed the derivation of relevant parameters from photometric *I*-band CCD images (Giovanelli et al. 1994, 1995, 1997c; Haynes et al. 1999b). In this paper, we focus on the derivation of the width variable from 21 cm H I line observations.

As discussed in Giovanelli et al. (1997c), the major observational cause of scatter in the TF relation is the error in the H I 21 cm line width. The scatter itself increases significantly among galaxies with smaller velocity widths. In practice, H I line widths are usually measured as the full width across the profile; the trick arises in deciding at what intensity level to perform the width measurement, and later, to account for the effects of resolution, smoothing, and noise. The choice of level has been rather arbitrarily made at some fixed fraction of the peak flux, or alternatively, of the mean flux. In the peak flux case, the next decisions consider whether to measure a single peak (the maximum over the whole profile) or the peak on each side of the (double-horned) profile. Historically, the measurement of a 21 cm line "velocity width" has varied from author to author. For example, Pierce & Tully (1988) always use a width measurement at a level of 20% of the single peak, whereas others such as

[1] The National Astronomy and Ionosphere Center is operated by Cornell University under a cooperative agreement with the National Science Foundation.

Aaronson, Huchra, & Mould (1980) and Mould et al. (1991, 1993) have used widths measured at 20% and 50% of the peak measured separately on the two horns. R. G., M. H., and their collaborators, whose widths have been adopted by a number of authors (see, e.g., Willick 1989; Fukugita, Okamura, & Yasuda 1993), have published width measurements favoring 50% of the mean flux, following the reasoning of Bicay & Giovanelli (1986). Moreover, spectra obtained for other purposes, such as the measurement of redshift or H I content, are typically of lower signal-to-noise and/or more heavily smoothed than is optimal for TF applications.

Since the global H I line profile samples the entire velocity field of the H I disk detected within the single-dish telescope beam, it is necessary to understand how the H I profile Doppler width relates to a true measure of rotation. In a companion paper, Giovanelli et al. (1998a, hereafter G98) explore the relationship between the H I profile widths, as measured here, with ones derived from optical Hα rotation curves. In this paper, we present width measurements derived from H I line spectra specifically for use in determining secondary distances via the TF technique and corrected appropriately to give a robust indicator of the true circular velocity.

In employing width measures derived from H I line profiles for TF applications, corrections for two broadening effects must be applied: first, the broadening of the observed width due to the combined effects of instrumental noise and resolution, and second, the broadening of the observed width due to the non-neglible contribution of noncircular motions, including turbulence, in the H I disk. Instrumental broadening depends on the frequency resolution of the spectrometer, the type of smoothing applied to the raw spectrum, and the signal-to-noise ratio (SNR). Any studies that attempt to employ the TF method to investigate the local peculiar velocity field over a wide area of sky will, of necessity, require the use of more than one radio telescope, thus requiring an understanding of the differences in spectrometers and processing software. Typical corrections for instrumental broadening and signal-to-noise range from 10 to 30 km s^{-1}; they are particularly critical in objects of small velocity width. Often, insufficient information is available in the literature to estimate accurately the corrections for such broadening. For this reason, the use of width values quoted from the older literature is likely to increase the scatter and possibly may induce systematic errors in TF applications, especially at the nearer distances where low luminosity, low width galaxies dominate the population.

As part of our project to obtain TF distances to nearby field spirals, we present in this paper a compilation of H I fluxes, velocities and velocity widths for galaxies for which we also have obtained *I*-band photometric images as presented in Haynes et al. (1999b). Complementary results for galaxies in nearby clusters have been presented previously by Haynes et al. (1997) and, for highly inclined late-type galaxies, by Giovanelli, Avera, & Karachentsev (1997a). For 881 galaxies, we have obtained new H I spectra using a variety of large single-dish radio telescopes. For an additional 320 galaxies for which spectra are available in a digital archive, we present newly derived H I parameters obtained from a reexamination of the spectra. In all cases, spectra have been analyzed using identical software, yielding a homogeneous and robust measurement of the H I velocity width and its error, specifically designed for TF applications. Additionally, observed H I widths available in the literature are converted to a similar scaling via regression relations derived through an analysis of spectra contained in the digital archive.

In § 2, we describe the new H I observations, and in § 3, we discuss the algorithm employed to measure the H I velocity widths. The final compilation for the 1201 galaxies is presented in § 4 for the spectral analyzed digitally. Recursion relations are derived to convert widths measured using other prescriptions, and corrected width measurements are presented for 72 additional galaxies in § 5.

2. NEW H I OBSERVATIONS

New H I observations of 881 galaxies were conducted with various radio telescopes during the period from 1988 June to 1996 February. Objects were selected from inclined spirals contained in the Uppsala General Catalog (Nilson 1973, hereafter UGC), the Catalog of Galaxies and Clusters of Galaxies (Zwicky et al. 1961–1968, hereafter CGCG), the Morphological Catalog of Galaxies (Vorontsov-Velyaminov & Arhipova 1968, hereafter MCG), the Southern Galaxy Catalogue (Corwin, de Vaucouleurs, & de Vaucouleurs 1985), or the ESO-Uppsala Survey of the ESO(B) Atlas (Lauberts 1982, hereafter ESO). For many of the galaxies, these observations represent the only available H I spectra. In some cases, the redshift was not known in advance. For other galaxies, new spectra have been obtained in order to provide better SNR or to make the spectrum available for our analysis. Included here are the H I properties of the galaxies that are included in the compilation of *I*-band photometric imaging properties presented by Haynes et al. (1999b). The discussion of the optical imaging sample selection is presented elsewhere (Wegner et al. 1999).

Observations have been conducted with the following five radio telescopes: the Arecibo 305 m telescope of the National Astronomy and Ionosphere Center, the 91 m and the 43 m telescopes of the National Radio Astronomy Observatory[2] at Green Bank, and the Nançay Radio Telescope of the Observatoire de Paris and the 100 m Effelsberg telescope of the Max Planck Institut für Radioastronomie. The choice of telescope was dictated by the sky location and angular size of the galaxy, and by the availability of the telescope. Nearly all observations were conducted in total power mode, with a position switching technique used to remove the instrumental baseline effects. At each telescope, calibration of the noise diodes was performed by conducting observations of radio continuum sources, and both the flux and velocity scales were further checked by observations of a sample of strong H I line emitting galaxies. Typical on-source integration times were dictated by signal-to-noise requirements and varies from as little as 5 minutes at Arecibo to as much as 2 hr with the 43 m and Nançay telescopes.

The main distinctions among the H I data set arise from differences in the sensitivities achieved with the different telescopes and differences in the resolution and bandwidth available with different spectral back ends. Hence, we discuss the H I data set according to the telescope and back end used.

[2] The National Radio Astronomy Observatory is operated by Associated Universities, Inc., under a cooperative agreement with the National Science Foundation.

2.1. *Arecibo* 305 m *Telescope Observations*

The Arecibo data presented here complement and extend the ones presented in Haynes et al. (1997) and Giovanelli et al. (1997a). New H I observations conducted at Arecibo made use of one of the two 40 foot long, dual circular polarization line feeds available for observing redshifted H I: the so-called "21 cm" and "22 cm" feeds. In terms of their beam characteristics and fundamental response, both feeds were similar and were as described in Haynes & Giovanelli (1984). The difference was that the 22 cm feed was tunable in frequency, that is, it could be refocused mechanically by means of a movable mount allowing control of its radial displacement. Both feeds had an instantaneous bandwidth (to half-power) of about 45 MHz, beamwidths of about 3.3 and a peak gain of 8 K Jy^{-1}. The 21 cm feed was mounted to achieve some particular peak response frequency, typically centered at around 1410 MHz. The 22 cm feed could be tuned remotely under computer control although the peak gain did fall considerably at frequencies below 1340 MHz.

The observing technique was the one adopted for most 21 cm observations made at Arecibo (see, e.g., Giovanelli & Haynes 1989), that is, constructing the total power difference spectrum obtained from alternating ON and OFF source observations of 5 minutes duration each. The OFF source observation was made to coincide with the track in azimuth and zenith angle of the ON source observation in order to allow removal of the instrumental baseline. The signal from each of the two orthogonal polarizations was fed to separate amplifiers in the back end chain. Further splitting of the output from each IF amplifier to separate quadrants of the 2048-channel autocorrelation spectrometer allowed for additional noise recovery in the case when all spectra were centered at the same redshifted frequency ("parallel-mode") or allowed for examination of spectra centered on different frequencies ("search-mode"). Typical Arecibo spectra covered 20 MHz with 512 frequency channels with a channel spacing of 39 kHz. In parallel mode, a single 20 MHz spectrum was constructed from the accumulated average of the four correlator quadrants (two spectra, two polarizations). In search mode, two separate 20 MHz spectra, one offset by 15 MHz from the other, were obtained by accumulating and averaging the two independent polarizations. Once a detection was obtained in search mode, subsequent observations, if needed, were conducted in parallel mode and then the spectra covering the same frequency range in both modes were combined to produce the final average.

In these and other observations, calibration of the noise diode has been performed by undertaking observations of strong sources from the 1400 MHz catalog of Bridle et al. (1972). In addition, several small angular diameter, H I-bright, narrow profile width sources were observed in order to examine the quantities derived from spectral measurements made with different telescopes, spectrometers, and spectrometer configurations.

Data reduction has been performed using the Arecibo ANALYZ-GALPAC analysis system. Initial reduction performed at the telescope included accumulation and flux calibration. All accumulated spectra have been reanalyzed to produce the derived parameters presented here.

2.2. *Green Bank* 91 m *Telescope Observations*

The 91 m telescope was one of the workhorse instruments for extragalactic H I line studies. Over the last 5 years of its lifetime, improvements to the feed and receiver system at *L* band had increased the sensitivity of the instrument to detect H I emission from galaxies significantly. In our last observing run in 1988 August, we detected over 500 galaxies in a 3 week observing period. The SFI galaxy project has the distinction of being the last one officially listed on a 91 m telescope schedule, for 1989 January. Unfortunately, that observing run was cancelled.

The observations presented here were conducted in several observing periods during the last years of the telescope's existence and are similar to those discussed in Haynes & Giovanelli (1991). All observations were made with a prime focus *L*-band receiver situated on the Sterling mount, allowing the tracking of sources for a duration of 4 minutes sec δ up to a maximum of 8 minutes. Observations were conducted in a total power mode, with OFF-source observations made at the same declination and following the same track in hour angle. Normally, one OFF scan was made either immediately preceding or following the ON source observation of equal duration. In some instances, when the declinations of neighboring ON source positions were within a few degrees, a single OFF source observation was shared by two ON source ones. The scheduling was arranged in order to maximize the number of sources while still retaining maximum tracking times at high declination. The NRAO *L*-band receivers consisted of dual polarization receivers allowing the simultaneous collection of independent signals in the front end. Observations were conducted in two modes depending on the advance knowledge of the galaxy redshift. Where the redshift was known, the Mark III autocorrelator was divided into two halves of 192 channels, each spectrum centered on the redshift of the target galaxy. Normally, a 10 MHz bandwidth was used in this "parallel" mode, except in the case of daytime observations where thermal deformation and solar interference caused a deterioration in the baseline quality. Observations were then conducted at 5 MHz. When the redshift of a galaxy was not known, the autocorrelator was divided into four quadrants of 96 channels each, with each 10 MHz band offset from the next by 7.5 MHz, giving a total velocity coverage of about 7000 km s^{-1}. Because this configuration provided a velocity resolution of about 44 km s^{-1} (after Hanning smoothing), inadequate for our purposes of obtaining redshifts and 21 cm line widths, once a detection was made, the autocorrelator was reconfigured for the next day's observations in the 2×10 MHz parallel mode with the spectrum centered on the galaxy redshift. Typical redshift search observations required about 3 days of search time and an additional 3–4 days of parallel mode integration to achieve adequate signal-to-noise. Because of the broadband requirement, no redshift searches were conducted during the daytime.

Initial calibration and accumulation of individual ON-OFF pairs was performed at the telescope using the NRAO UNIPOPS package. Spectra were then exported into the ANALYZ-GALPAC format for further analysis.

2.3. *Green Bank* 43 m *Telescope Observations*

Observations with the NRAO 43 m telescope at Green Bank were made in eight separate observing periods, three in 1989, three in 1992, one in 1995, and one in 1996. The latter two make use of the scheme to obtain accurate H I fluxes discussed in van Zee et al. (1997) and Haynes et al. (1998). The front end was identical to that used on the 91 m telescope, but at prime focus on the 43 m telescope, an even

better system noise of 20–22 K at zenith was attained. At 21 cm, the beamwidth of the 43 m telescope is about 21′ and the gain is about 0.25 KJy^{-1}. Initially, we intended to use the 43 m telescope only to survey the region south of that of the 91 m—that is, declinations south of $-18°$. However, after the collapse of that telescope, we extended the range northward toward the equator. In addition, the last two observing runs were used to resurvey large angular diameter galaxies ($a > 3'$) for which digital spectra were not available. A further constraint on targets of this last program was that they could have no known companions that might be contained within the 21′ beam of the 43 m telescope.

The observations with the 43 m were conducted in a typical total power mode of alternating 10 minute ON and OFF scans. Most spectra were obtained with a correlator configuration set so that each polarization was fed to a half-correlator, giving a spectrum of 512 channels over a maximum bandwidth of 10 MHz. Typical integration times were 2 hr per galaxy (ON plus OFF source). Calibration of the noise diode was achieved by comparison with continuum sources of known flux density from Ott et al. (1994). For the 43 m telescope, no correction has been applied for gain variations with zenith angle, but because of the large zenith distances of these southern objects, a correction for atmospheric extinction has been applied (Williams 1973; van Zee et al. 1997).

Accumulation of the individual ON-OFF pairs and flux calibration was made using the NRAO UNIPOPS package. Final analysis was done using the Arecibo ANALYZ-GALPAC software.

2.4. *Nançay Radiotelescope Observations*

New observations were conducted with the Nançay radiotelescope in several observing periods between 1990 and 1993. Spectra were obtained in a total power mode with alternating ON and OFF-source scans of 2 minutes duration made covering the same hour angle. Spectra were obtained for both polarizations (horizontal and vertical on the sky); further reduction of noise in the back end was achieved by feeding each polarization to separate quadrants of the 1024-channel autocorrelation spectrometer. Each spectrum consisted of 256 channels covering a total bandwidth of 6.4 MHz. In most cases, the redshift was known prior to observation from optical means. In a few of the galaxies, detection was achieved using a redshift search technique by which four separate 6.4 MHz spectra were produced, successive ones offset by the equivalent of 1200 km s^{-1} from the preceding. The number of ON-OFF pairs was generally limited to exclude hour angles greater than ± 40 minutes, beyond which the gain of the telescope falls. The individual ON-OFF pairs were accumulated with initial calibration and averaged using the standard routines for data reduction available at Nançay (RTF or DAC). Further calibration and extraction of profile parameters was performed using specially developed modules of the Arecibo Observatory ANALYZ-GALPAC analysis system. Final spectra were Hanning smoothed.

The Nançay radiotelescope consists of a fixed spherical antenna and a steerable flat plate that together produce an elongated beam on the sky. Half-power dimensions of the beam at 21 cm are 4′ in R.A. and 22′ in declination; this last figure increases for $\delta \geq +30°$, but all of our program galaxies lie south of that limit. Tracking through hour angles less than about ± 35 minutes is accomplished via a movable feed cabin. A series of calibration observations were conducted in order to examine the variation with both hour angle, elevation angle and frequency of the calibration noise diode. Using a routine kindly provided by the late G. Bourgois, we recorded the voltage deflection for both polarizations simultaneously at two frequencies in a 3 minute drift mode across sources of strong continuum flux taken from BDFL, with the calibration diode fired at both the beginning and the end of the scan. We then fitted a baseline to the observed response and derived for each polarization of each scan at each frequency relative values of the source, noise diode and system temperature. By conducting observations of many sources covering a variety of declinations close to transit, Fouqué (1982) derived the variation in the telescope gain over all declinations. Since all of our primary sources are located south of the equator, we were primarily interested in the gain correction in that region, and only confirmed Fouqué's findings. Note that because of the design of the Nançay radiotelescope, the gain is at a maximum and nearly constant over the declination range $-20° < \delta < +20°$.

Once the gain correction for declination was applied, we then investigated the variation as a function of hour angle of the telescope response for five different sources over the complete hour angle track at a single frequency setting of 1400 MHz. Gain variations are not seen over the inner $\pm 40^{\min}$. A further correction was applied for the variation of the calibration diode with frequency. For four sources, noise diode variations were measured in steps of 5 MHz using a bandwidth of 5 MHz over the range from 1380 to 1420 MHz. A mean variation was adopted to correct the observed fluxes to true ones since accumulation of individual polarizations was performed automatically, without benefit of this calibration, at Nançay.

In addition, line observations of a number of galaxies with previously published H I parameters were made in order to compare flux and velocity scales. Excellent agreement was found, proving the efficacy of our calibration and analysis procedures and the routines used to reconstruct the data in standard ANALYZ/GALPAC format.

Chamaraux provided access to data obtained in his 21 cm line survey of MCG galaxies in the southern equatorial strip so that profile parameters could be extracted using the same algorithms as applied to the newly obtained spectra.

2.5. *Effelsberg* 100 m *Telescope Observations*

Observations with the 100 m telescope of the Max Plank Institut für Radioastronomie in Effelsberg, West Germany, were conducted during two observing periods in 1989 October and November. The standard *L*-band receiver is characterized by a system temperature on sky of about 45 K at zenith. The two orthogonal polarizations were each fed to separate correlator halves, producing two independent spectra of 512 channels each. A variety of different total bandwidths were used, depending on the time of day and the availability of redshift measurements. Solar interference was particularly severe and restricted the usable bandwidth to a maximum of 6.25 MHz. At night, especially on weekends when the radio frequency interference (RFI) was quieter than normal, redshift searches were conducted over a total bandwidth of 25 MHz. Better results were obtained under more normal circumstances with bandwidths of 12.5 MHz or less.

Observations were conducted in a total power mode with alternating ON and OFF source scans normally of 10 minutes duration each. The initial calibration, accumulation and averaging of ON-OFF pairs was performed using the standard MPIfR package TOOLBOX. Additional calibration of the noise diode including investigation of the frequency response was conducted by making continuum observations of a number of sources chosen from Bridle et al. (1972). Further calibration of the spectra for atmospheric correction and noise diode variation with frequency was performed during the phase of translation into export format for compatibility with the Arecibo Observatory ANALYZ-GALPAC analysis system. Baseline fitting, removal, and parameter extraction were all performed using the latter package.

The RFI environment in western Europe is particularly hostile and certain frequency ranges, even at low redshift, were completely useless for observational purposes. In some cases, the interference was sufficiently catastrophic that observations in that band had to be abandoned; in other cases, significant editing of data using interpolation to replace bad channels was performed. Cases of interference removal and possible or likely interference contamination are mentioned in § 4.1.

2.6. *A Digital Archive*

In addition to the new observations, we have also constructed a digital archive of H I line spectra observed by us and our collaborators over the last 10–15 years. The availability of the spectra in a standard digital format (the ANALYZ/GALPAC "history" file format) has permitted us to reexamine data obtained long ago and for other purposes. Accumulated and averaged spectra for some 10,000 galaxies are available for reprocessing. In addition to the new observations, we have reexamined the H I line data for 320 galaxies also included in the optical imaging sample of Haynes et al. (1999b). In all cases, the reprocessing has mimicked that used for the newly obtained data.

Since smoothing increases the width measurement systematically, an improvement in the current data set is that, in the reanalysis, we have applied only a single Hanning (convolution with a three-point 0.25:0.50:0.25 function) smoothing in reprocessing the available data. In some cases of low signal-to-noise, it is necessary to apply the Hanning plus boxcar (convolution with a three-point equal weight function) smoothing. In each case, the observed width is later modified by means of a statistical correction that takes proper account of the smoothing applied to the spectrum. A record of parameters required for applying corrections to the observed width is maintained through our analysis process. H I line systemic velocities and widths have been measured in a variety of ways including using the algorithm described in § 3. Final parameters derived from the reanalysis include fluxes, systemic velocities, and velocity widths. Furthermore, spectral resolution, smoothing parameters, the rms noise per channel, and peak SNR are also recorded for use in correcting for instrumental broadening.

For 51 objects, we have obtained spectra with more than one telescope. In all cases, velocities and widths are in agreement within estimated errors and fluxes, corrected for beam effects, agree to within 20%.

The final result of the reanalysis is a homogeneous set of H I line recessional velocities and widths that we use for TF applications to derive the peculiar velocities of the galaxies in the optical imaging sample.

3. 21 CENTIMETER LINE WIDTHS

As mentioned previously, a main objective of this work is to obtain uniform measurements of the rotational width parameter from H I line spectra for the specific purpose of applying the TF relation. Past measurements of H I line width have not been developed necessarily with TF applications in mind, and the definition of the H I line width measurement has been quite arbitrary. Here we review the H I line width measurement algorithm developed for use in TF applications. Further discussion of its relationship to measurements made from optical rotation curves is presented in G98. In this section, we briefly review the adopted width measuring algorithm and the need for corrections for instrumental and turbulent broadening.

3.1. *A Robust Width Algorithm*

H I line width measures have historically been made at a fixed fraction of the peak or mean flux. Among others, Bicay & Giovanelli (1986) have shown that measurements at relatively large fractions of the peak are sensitive to noise in the case where the SNR, typically defined as the ratio of the peak flux to the rms noise per channel is not very high (say, of order 10 or less). Schneider et al. (1986) and Corbelli & Schneider (1997) discuss the advantages of using a measure at a larger percentage of the peak signal, while Bicay & Giovanelli (1986) point out that the higher up the measurement is made, the more sensitive is the resultant width to noise at the peak location.

For the present study, simulations were performed on synthetic profiles to investigate the change in gradient of the rise of intensity on each side of the profile as a function of intrinsic slope of the profile, the applied smoothing, and noise. To simulate the effects of the finite autocorrelator channel width characteristic of the spectrometers used, the resolution is modeled as a convolution with a Gaussian of HPFW of 1.2 times the channel separation. The results of many simulations were examined in order to establish the "best" algorithm for measuring widths as well as to obtain corrections for observed widths as functions of SNR, resolution and the slope of the profile sides. Algorithms that prove effective on simulated data were then applied to the entire data set interactively, because "real" data are never quite like the simulations.

The adopted width measuring algorithm is designed to give a better estimate of the maximum rotational velocity and makes use of the shape of the profile rather than just the peaks or mean intensities. As discussed by Schneider et al. (1986), Corbelli & Schneider (1997), and G98, measurements of the width at higher flux levels on the two horns map better the maximum rotational velocity, presumably the parameter of importance for TF applications. The width, referred to hereafter as W_{21}, is defined as the full width across the profile measured at a level of 50% of each horn but identifying the appropriate level by fitting a polynomial between the levels of 15% and 85% of the respective horn to each side of the profile. In this application, the 50% level is measured from the fitted polynomial, not on the individual spectral points. By default a straight line is fitted to the profile sides, but should the fit be poor, the user is given the option of fitting a higher order (second degree)

polynomial. Figure 4 of G98 illustrates the application of this method; those authors also discuss the comparison of widths measured for a set of galaxies with both H I profiles and Hα rotation curves. The adopted algorithm includes a better estimate of the formal error on the velocity width, making use of the full details of the digital spectrum. It should be noted that this algorithm is now incorporated both in the Arecibo ANALYZ-GALPAC package and the UNIPOPS spectral line reduction package in use at the National Radio Astronomy Observatory.

As noted by G98, this algorithm may fail in measuring widths when profiles are not double horned. At low SNR, the peaks may be hard to identify; a threshold of S/N $\simeq$ 7 appears to be optimal. Distorted or grossly asymmetric profiles cannot be used. Single-horned profiles arise in three cases: (1) when galaxies are viewed nearly face-on so that Doppler broadening is minimized; (2) in dwarf irregular galaxies, where the rotation motion is not resolved by the spectral resolution; (3) asymmetric galaxies of the "missing horn" class. Because the current sample targets inclined, spirals, the number of galaxies exhibiting single-horned profiles is very small: 15 of the 1201 objects. Widths are estimated for these galaxies by examination of the individual spectra. For galaxies with asymmetric profiles (missing horns), a width measurement is estimated by folding the prominent horn about the systemic velocity. For Gaussian profiles, the measurement at the 50% of peak value underestimates the maximum rotational velocity (G98); we estimate the correction for each galaxy after examining the slope of the profile on each side. In these cases, the error on the width is also increased to reflect the uncertainty.

3.2. *Corrections for Signal-to-Noise, Instrumental Broadening, and Redshift*

The adoption of a single, robust width estimator is the first step in producing homogeneous velocity widths. Each width must be corrected for the instrumental effects of smoothing and nonzero channel width that broaden the profile on each side. Over the last 20 years, nearly all of the spectrometers used for extragalactic H I line observations have been either one- or three-level autocorrelators in which spectral data are obtained from the multiplication of the clipped voltage signal by a delayed replica of itself through a succession of accumulated lags, i.e., the autocorrelation function. Nearly always, the spectral points are sampled at fixed frequency intervals, referred to as the channel separation (in frequency units). Corrections for the instrumental broadening are therefore dependent on the spectrometer channel separation (finally in km s^{-1}), the degree of smoothing, and the shape and SNR of the spectrum. We define the "lag" as the broadening of the profile on a single horn produced by the smoothing and nonzero channel width. Estimates of the appropriate corrections as a function of the intrinsic slope of the horn, the applied smoothing, and the SNR ratio were derived from Monte Carlo simulations. For a channel separation δv in Hz giving a corresponding δV in km s^{-1} and a SNR defined as the ratio of the peak intensity to the rms noise per channel, the lag, in units of the channel separation, is then computed according to the SNR and degree of smoothing by the relations given in G98.

Because of the algorithms used to convert frequency to velocity, an additional correction for redshift stretch must be applied to derived widths by reducing the width corrected for instrumental broadening and SNR by a factor of $(1 + z)^{-1}$.

In this paper, we present H I widths, corrected for signal-to-noise, smoothing, and instrumental broadening, along with an error on the velocity width that includes a contribution for the instrumental effects. This latter term is taken, from simulations, to be equal to one-quarter of the broadening correction and is added in quadrature to the estimated error from application of the width measuring algorithm. In final applications of the TF relation, H I line widths must also be corrected for turbulent broadening and for viewing angle. The turbulence correction is discussed in G98.

It should be remembered that the application of the TF technique requires somewhat different observational strategies than, for example, the derivation of galaxy redshifts. Because for TF applications a high SNR is desired, longer integration times are required to attain constant SNR for galaxies with larger observed velocity widths. This practice will be seen in the examination of the characteristics of the H I data set presented in the next section.

4. DATA COMPILATION

All spectra in the digital archive, including new ones, have been reanalyzed using the Arecibo ANALYZ-GALPAC package following a uniform processing path. We present in Table 1 the results of the analysis for the 1201 galaxies whose digital spectra have been examined. The table is

TABLE 1

PROPERTIES OF GALAXIES DERIVED FROM SPECTRA IN DIGITAL ARCHIVE

Number (1)	Other (2)	α(1950) (3)	δ(1950) (4)	$a \times b$ (5)	T (6)	S (7)	S_c (8)	rms (9)	SNR (10)	$V_\odot$ (11)	W_{21} (12)	W_c (13)	ϵ_W (14)	Codes (15)
400001.....	M−101024	00 00 01.0	−03 59 20	2.0 × 1.5	4	3.45	3.65	2.23	9.8	6463	348	333.5	3.5	mHG
14	478-019	00 01 01.2	+22 55 19	1.9 × 1.0	5	6.98	8.61	2.15	13.5	7254	348	330.3	5.6	bHG
19	NGC 7817	00 01 24.9	+20 28 18	4.0 × 1.1	4	18.94	19.25	6.95	11.4	2310	388	380.0	5.2	kHG
24	478-020	00 01 39.6	+22 18 40	1.2 × 0.8	5	4.35	4.94	1.73	17.8	4444	179	168.2	2.9	bHG
25	M+101020	00 01 51.6	+05 53 53	1.1 × 0.3	5	3.61	3.98	1.91	11.0	5071	277	261.9	9.4	bHG
27	408-020	00 01 55.6	+05 34 00	2.2 × 1.2	5	8.91	11.59	2.45	21.6	3113	215	205.3	3.6	bHG
41	M+401022	00 03 23.0	+22 12 47	1.2 × 0.3	5	3.57	3.97	1.15	16.8	6597	256	242.0	3.7	bHG
51	408-031	00 04 06.6	+04 50 06	1.1 × 0.7	4	2.17	2.43	0.94	13.4	5371	293	278.5	3.1	aHG
53	456-031	00 04 15.4	+19 02 37	1.4 × 0.8	4	1.98	2.29	1.49	9.3	7894	160	144.2	6.7	bHG
57	NGC 1	00 04 41.3	+27 25 50	1.8 × 1.2	3	11.75	14.55	4.55	11.0	4554	317	301.7	5.7	bHG

NOTE.—Table 1 is presented in its entirety in the electronic edition of the Astronomical Journal. A portion is shown here for guidance regarding its form and content.

available in its entirety electronically; the example printed here contains only the first lines. Figure 1 shows a sample of the H I spectra, presenting here those of the first 16 galaxies listed in the table. The smoothed curve in each profile is the polynomial baseline subtracted from each spectrum before derivation of the emission properties. Strong, typically narrowband RFI is present in many of the spectra. Similar montages of the additional profiles can be obtained by contacting M. P. H.

Details of the entries in Table 1 are as follows:

Column (*1*).—Entry number in the UGC (Nilson 1973), where applicable, or else in our private database, referred to as the Arecibo General Catalog (AGC).

Column (*2*).—NGC or IC designation, or other name, typically from the CGCG, ESO, or MCG. Where used, the designation in the latter is abbreviated to eight characters.

Columns (*3*) *and* (*4*).—Right ascension and declination in the 1950.0 epoch, either from the literature or measured by us on the POSS-I. Typically, the listed positions have 15″ accuracy.

Column (*5*).—The blue major and minor diameters, $a \times b$, in arcminutes, either from the UGC or ESO catalogs or as estimated by us on the POSS-I.

Column (*6*).—The morphological type code following the RC3 (de Vaucouleurs et al. 1991) system. Classification comes either from the UGC or ESO catalogs or from our own visual examination of the POSS-I prints.

Column (*7*).—The observed integrated 21 cm H I line flux $S = \int S_V \, dV$ in Jy km s^{-1}.

Column (*8*).—The corrected integrated 21 cm H I line flux S_c, also in Jy km s^{-1}, after corrections applied for pointing offsets (Arecibo only) and source extent following Haynes & Giovanelli (1984).

Column (*9*).—The rms noise per channel of the spectrum, rms, in mJy.

Column (*10*).—The emission profile signal-to-noise ratio (SNR) taken as the ratio of the peak flux to the rms noise.

Column (*11*).—The heliocentric velocity $V_\odot$, in km s^{-1}, of the H I line signal, taken as the midpoint of the profile at the 50% level also used to measure the width (see below).

Column (*12*).—The full velocity width W_{21}, in km s^{-1}, of the H I line, uncorrected for redshift or other effects, using the measurement algorithm discussed in § 3.1.

Column (*13*).—A corrected velocity width W_c, in km s^{-1}, which accounts for redshift stretch, instrumental broadening and smoothing. Note that this width is not rectified for

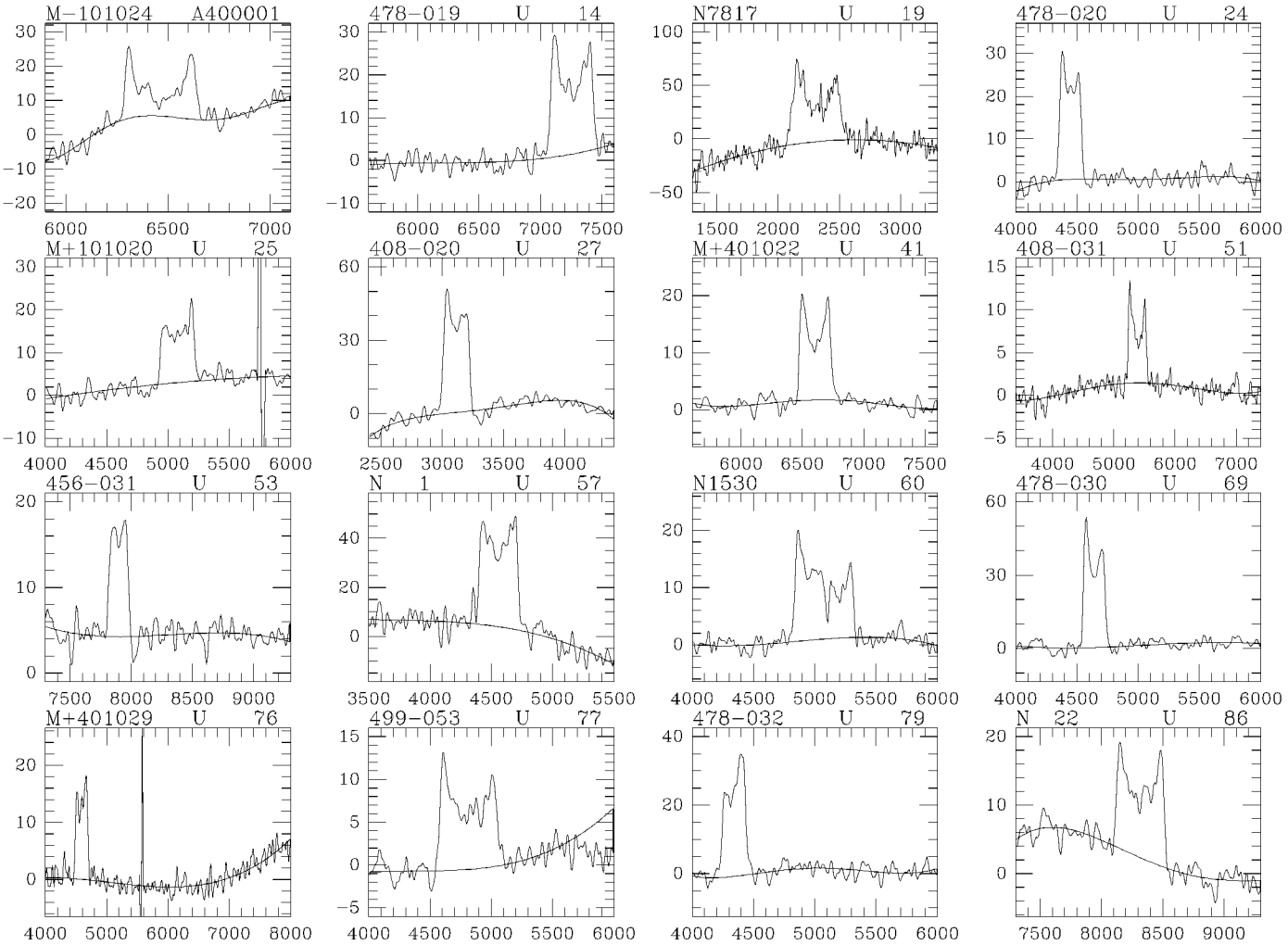

FIG. 1.—A sample montage of spectral profiles for the first 16 galaxies included in Table 1. The *x*-axis is heliocentric velocity in km s^{-1}; the *y*-axis is flux in mJy.

viewing angle. A correction for turbulent broadening should also be applied for TF applications.

Column (14).—The estimated error on W_c, ϵ_w, in km s^{-1}, taken to be the sum in quadrature of the measurement error and the estimated error in broadening corrections. The estimated error on the velocity itself, ϵ_V, can be approximated as $\epsilon_w/2^{1/2}$.

Column (15).—A series of codes indicating the correlator mode, smoothing, width quality, and data source.

The first code refers to the origin and configuration of the spectrum from which parameters are derived: (a) Arecibo spectrum, 20 MHz/512 channels; (b) Arecibo spectrum, 10 MHz/252 channels; (c) Arecibo spectrum, 10 MHz/512 channels; (d) Arecibo spectrum, 10 MHz/504 channels; (e) Arecibo spectrum, 5 MHz/512 channels; (f) Effelsberg spectrum, 25 MHz/512 channels; (g) Effelsberg spectrum, 12.5 MHz/512 channels; (h) Green Bank 91 m spectrum, 10 MHz/192 channels; (i) Green Bank 91 m spectrum, 5 MHz/192 channels; (j) Green Bank 43 m spectrum, 20 MHz/512 channels; (k) Green Bank 43 m spectrum, 10 MHz/512 channels; (l) Green Bank 43 m spectrum, 5 MHz/512 channels; (m) Nançay spectrum, 6.4 MHz/256 channels.

The second code is the smoothing code: (H) single Hanning only; (B) Hanning plus three-channel boxcar.

The third is a qualitative assessment of the quality of the profile for TF applications: (G) good; (F) fair; (S) single peak; (P) poor quality for TF applications; (M) marginal detection; (C) confused. Velocity widths measured from profiles classified as good detections should be useful for TF applications; those measured on profiles denoted "F" should be used with caution. Because the width measuring algorithm is designed for application to two-horned profiles, the widths measured on single peaked profiles should also be used with caution, as they may underestimate the true rotation width. Widths in the last three categories cannot be used for TF purposes. A designation of marginal detection is given to those cases in which the signal has not been verified through adequate reobservation. Confusion is identified only when contamination from another galaxy in the beam is certain.

Another code follows where applicable that indicates inclusion in other compilations: "c" for the cluster compilation of Giovanelli et al. (1997c), "a" for the study of asymmetry in H I profiles by Haynes et al. (1998).

A final asterisk (*) in this column indicates the presence of a comment for the object in the following notes to Table 2.

4.1. *Notes to Table 1*

U100.—Interference excised from profile.

U229.—Strong RFI on spectral profile; parameters uncertain.

TABLE 2

REGRESSION RELATIONS: $W_{21} = aW_o + b$

Width Definition	a	b (km s^{-1})
50% of mean	+0.00925	10.8
50% of peak	−0.0106	1.4
20% of peak	+0.0003125	20.5
50% of two peaks.....	+0.00275	0.8

U256.—Poor; parameters very uncertain.

U271.—Sloped sides.

A400271 = M-202049.—Low SNR.

A400274 = M-202051.—Also Effelsberg spectrum; parameters agree.

U346.—Serendipitous detection of an H I signal in "off" at 5400 km s^{-1}, unidentified, at α, $\delta(1950) = 00^h38^m16^s.6$, $+31°40'$. No obvious identification on POSS.

A400296 = M-102038.—Noisy sides.

A400367 = M-103005.—Asymmetric, noisy. MCG-1-03-004 at 6.′4, redshift unknown.

A400375 = M-103010.—Marginal detection at optical velocity.

A400411 = N268.—Unusual profile with central peak.

U565.—Profile includes separate feature from U566 at 3.′6 at higher velocity.

U632.—Marginal detection at RC3 velocity; also CGCG 501-064 at 1.′6, same velocity.

A110090.—Interference excised from profile.

U886.—Asymmetric.

U914.—Flux with 21′ beam of 43 m telescope is 31.98, adopted as S_c matches well the Arecibo flux without need for size correction.

U1070.—Asymmetric.

A110417.—Extremely marginal detection near optical velocity.

U1305.—Asymmetric.

A410384.—Also 93 m profile; parameters comparable. Asymmetric. Two small galaxies of unknown z within 3′ and within Nançay beam.

U1526.—Confused with N799 at 1.′8; blended profile.

U1554.—Use 43 m telescope flux 32.61 for S_c; other parameters from Arecibo. 43 m telecope spectrum yields $V_\odot = 2098$ km s^{-1} and $W_{21} = 257$ km s^{-1}, in excellent agreement with Arecibo data.

U1567.—Marginal detection at optical velocity.

U1612.—Interference present within emission range.

A420056 = N873.—Single-peaked profile.

U1834.—Single-peaked profile.

U1862.—Single-peaked profile.

A120257 = 462−013.—N924 = U1912 at 3.′1 is probably feature at ~4600 km s^{-1}.

A420143 = M-207033.—Possibly blended but uncertain. Three small galaxies of unknown z within 2′.

U2135.—Interference excised from profile.

A420244 = N1084.—43 m flux is 68.21.

U2313.—Marginal detection at optical velocity, in agreement with Theureau et al. (1998).

U2586.—Marginal detection at optical velocity. Theureau et al. (1998) have firm detection with wider width.

U2617.—Profile appears disturbed; I309 at 5.′1, within beam: blend? interaction?

A430121 = M-209021.—Poor baseline subtraction.

U2736.—Marginal detection near optical velocity.

U2742.—Marginal detection near optical velocity.

U2801.—Severe RFI excised from profile. Parameters report here in conflict with those reported by Theureau et al. (1998).

U2888.—Asymmetric profile; confused with CGCG 508−002 at 2′.

A440292 = N1618.—Broad, low flux shoulder on low velocity side; parameters uncertain.

U3405.—Pair with U3410 ($V_\odot = 4026$ km s^{-1}) at 2′; blend, but width and velocity perhaps recovered.

A 25174 = 557 G 2.—Confused with 557 G 1 at 1.4. Both Nançay and Effelsberg observations.

U3606.—High order baseline.

A480050 = M-222023.—Spectrum appears disturbed, especially on low velocity side; yet no visible optical counterpart.

U4628.—High order baseline.

U4640.—High order baseline.

U4719.—In group with several fainter companions; profile slightly broadened by interaction or blend on high velocity side; width recovered. Observed at both Effelsberg and with 92 m telescope. Parameters agree.

A490006 = N2763.—43 m telescope flux is 16.70, perhaps more reliable than 92 m telescope flux.

A26380 = N2821.—Noisy profile.

U4961.—Confused. Triple with I2458 at 1.9 and N2814 at 3.4.

U5029.—VV 106a, Arp 300b: interacting system, disturbed; blended profile.

U5303.—43 m flux of 21.13, adopted for S_c.

A 26740 = 499 G 26.—disturbed profile; however, W_{21} reported here is more reliable than value of 238 km s^{-1} reported in Giovanelli et al. (1997c).

U5522.—Measured flux within 3.3 Arecibo beam is 30.56.

A200399 = A1016−13.—Marginal detection at optical velocity but possibly confused with U5665 at 1.5.

U5742.—Strongly asymmetric chaotic image; asymmetric spectral profile.

A500163 = N3321.—43 m telescope flux is 21.39, adopted for S_c.

A 27441 = 501 G 75.—Discrepant velocity compared with MF96 and Theureau et al. (1998). 10 MHz spectrum of low S/N obtained with 43 m telescope shows two features at 5200 and 4700 km s^{-1}.

U5914.—In group with U5092 (E) at 10′, U5911 (S0) at 6.5; disturbed spectrum?

A 27566 = 569 G 14.—43 m telescope flux is 28.12, adopted for S_c.

A500216 = N3456.—Blend; extraction of width uncertain.

U6126.—92 m telescope flux is 49.39.

U6209.—Very asymmetric profile; uncertain extraction of width.

A 27904 = 493 G 10.—Low S/N profile; width appears OK.

U6583.—097−027 at 2′; blend resolved, parameters reliable.

A210681 = 097−093.—Marginal detection at optical velocity. Several objects in beam.

U6802.—U6815, large spiral at $V_\odot = 975$, is at 6.2; blended profile can be resolved.

A 28198 = N3981.—Profile edge slopes nonlinearly, increasing uncertainty in measure of width.

U7054.—Optical image larger than beam; H I profile probably does not yield full rotational width.

A 28382 = 441 G 14.—Profile may be blended; spiral companions within 3′ in R.A., of unknown velocity. Note also the large spiral I764 at 20.6 north at similar velocity.

U7171.—In pair with small companion. Appears confused.

U7399.—Blend with companion in beam (probably U7408 at $V_\odot$ 462 at 30′); kinematic parameters recovered, albeit with increased uncertainty.

U7412.—U7418 = N4302, large edge-on Sc at nearly same z, is at 2.4; blended profile, parameters suspect.

A 28485 = 506 G 4.—Marginal detection at optical velocity, confirmed by Theureau et al. (1998).

A520051 = N4348.—43 m telescope flux is 14.75, adopted for S_c.

U7695.—Spectrum partly confused with local H I from Milky Way.

U7852.—Profile has no horns.

U7870.—92 m telescope flux is 51.20.

A520163.—Nançay flux is 26.97, $V_\odot = 4298$, $W_{21} = 428$ km s^{-1}.

U7993.—Blended profile; unknown companion. Width extraction OK; discrepant optical $V_\odot = 3035$ km s^{-1}.

A 28906 = 507 G 29.—Second feature at $V_\odot \sim 3480$ km s^{-1} probably due to one of two small spiral companions within 2′ in R.A. of galaxy, also seen (prominently, as expected) in GB 43 m spectrum.

U8036.—Unidentified, noninterfering feature at $V_\odot = 422$, $W_{21} = 25$ km s^{-1}.

A221149 = 160−034.—Marginal detection near optical velocity. Several objects in beam.

U8353.—In group with several companions; U8354 at 3.2 on edge of beam; partial blend.

U8365.—Feature at 600 km s^{-1} of unknown origin.

U8534.—Asymmetric profile; no optical evidence of disturbance.

U8787.—Triple-peaked profile; Irr/pec companion at 2.7: blend? Other possibility: $V_\odot = 4382$ km s^{-1}, $W_{21} = 243 \pm 5$ km s^{-1} ($v_{\rm opt} = 4356$ km s^{-1}).

U8967.—RFI close to high velocity side of galaxy profile; parameters OK.

A 30457 = 511 G 5.—Marginal detection near optical velocity.

U9115.—Sbc companion at 0.5; spectrum of mediocre quality, maybe blended.

U9176.—Arp 286. In triple with U9175 at 4.2 and U9172 at 6.8; blend.

U9245.—Single-peaked profile; width determination difficult.

U9328.—Arecibo flux in inner 3.3 is 15.48.

U9476.—S0 companion at 3.3; profile may be blended.

U9681.—Spiral companion (U9684) at 2.1; blend.

A 31083 = 513 G 26.—Spiral companion at 1.2; either disturbed or blended spectral profile.

A550029 = N5878.—43 m telescope flux is 31.61, adopted for S_c.

U9802.—In pair with companion; confused.

U9817.—Companions at 3 and 5.5; either disturbed or blended spectral profile.

A 31180 = 449 G 10.—Asymmetric profile; In triple. Parameters uncertain.

U9940.—Appears blended but no obvious companion.

U9948.—In N2985 (at 13.6) group, with U9961 at 6.2 and N5976 t 8.4; blend?

U10445.—43 m telescope flux from Haynes et al. (1998) is 29.54, adopted for S_c.

U10458.—Very asymmetric profile; flux ratio between horns is ~ 10.

U10641.—Arp 293. Marginal detection, probably confused with U10647 at 4.5 and N6285 at 4.8.

U10661.—Asymmetric profile; parameters uncertain.

U11286.—Asymmetric profile but parameters might be OK, or possibly confused with I4763 at 9.4.

U11320.—Companion at 1′; both features in spectrum,

no confusion.

U11390.—Asymmetric profile; parameters uncertain.

U11459.—92 m telescope flux is 20.14, $V_\odot = 3125$, $W_{21} = 362$ km s^{-1}.

U11475.—Sloped sides; parameters uncertain.

A600180 = M-2-53-022.—Marginal detection; no optical velocity.

U11919.—Second, noninterfering feature in profile?

A320193 = 452−007.—Asymmetric trapezoidal profile; spiral companion at 2.′7: interaction/blend?

U12075.—In interacting group with U12073 at 3′; disturbed/blend?

A620203 = M-2-58-011.—Double system of spirals, separation 0.′6, in strong interaction; confused so that extraction of width is impossible.

U12321.—Galaxy emission superimposed on broad and roughly Gaussian pedestal of emission of unclear origin.

A630027 = M-2-59-001.—Marginal detection near optical velocity.

U12421.—Second feature in spectrum is probably RFI.

U12459.—Second feature at higher velocity is I5297 at 8.′6.

U12543.—In group with U12545 at 2.′5, U12546 at 3.′5

A330598 = 476−080.—Marginal detection at optical velocity.

A330721.—In pair; asymmetric, probable blended profile.

A330781.—in dense part of cluster; several galaxies in close vicinity; blend?

U12780.—part of Arp 86, interacting pair, M51-like; profile perturbed? Width probably slightly overestimated.

U12787.—Asymmetric profile, perhaps disturbed, but no visible optical companion in vicinity.

U12888.—Several fainter companions in vicinity; disturbed/blended profile?

5. CHARACTERISTICS OF THE CURRENT DATA SET

Figure 2 summarizes via histograms the rms noise per channel, SNR, H I flux, velocity, observed velocity width W_{21}, and error on the width W_c, ϵ_w. The completeness of the SFI sample will be discussed in more detail elsewhere (Wegner et al. 1999) but several points are worthy of note.

In Figure 2*a*, the galaxies are separated in the histogram by the telescope used to obtain the final spectrum. The shaded area indicates spectra obtained at Arecibo (497 galaxies), while the open area contains galaxies observed elsewhere (614 galaxies). The separation demonstrates the superior sensitivity of the Arecibo telescope. The mean rms noise per channel attained at Arecibo is 1.7 ± 0.9 mJy, whereas for the remainder of the sample, it is 5.7 ± 3.6 mJy. In fact, because Sbc–Sc galaxies are generally rich in H I, this survey is not H I-sensitivity–limited. Within the prime SFI volume ($cz < 7500$ km s^{-1}), Sbc-Sc galaxies are easily detectable with reasonable integration times.

At the same time that the detection of H I in such objects is relatively easy, the application of the H I line profile for TF width measurements requires the spectra to be of higher signal-to-noise than necessary for other purposes. As can be

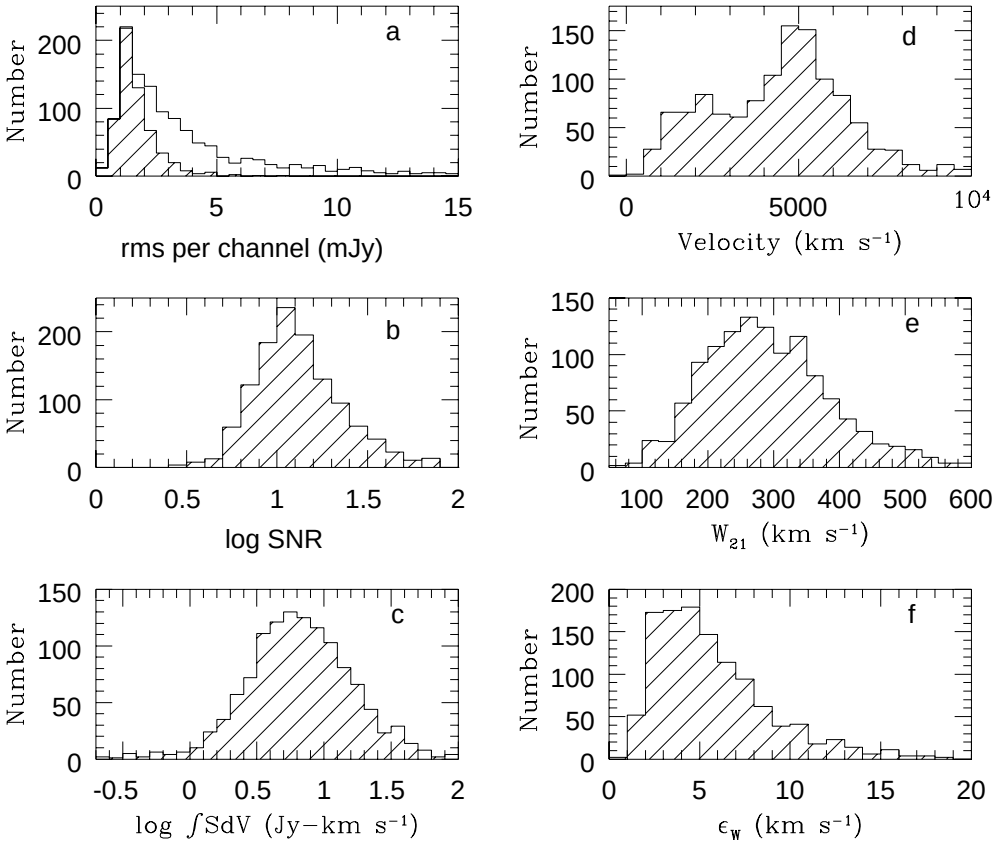

FIG. 2.—Histograms of the H I spectra and derived properties of the galaxies included in Table 1: (*a*) rms noise per channel, rms, in mJy; (*b*) peak signal to rms noise ratio, SNR, in logarithmic units; (*c*) observed H I line flux, $S = \int S\, dV$, in Jy km s^{-1}; (*d*) observed heliocentric velocity, $V_\odot$, in Jy km s^{-1}; (*e*) observed H I line width W_{21}, in km s^{-1}; (*f*) error on the corrected H I line width ϵ_W, in km s^{-1}.

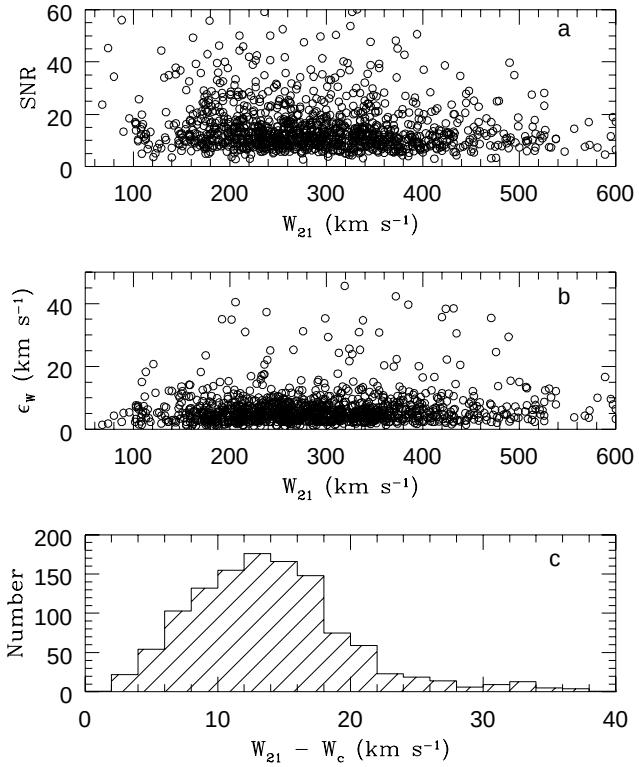

FIG. 3.—Characteristics of width measurements. The top panels show the variation of observed H I line width W_{21} with SNR (*a*) and estimated error on the width ϵ_W (*b*). Panel (*c*) displays the histogram of the corrections, $W_{21} - W_c$, applied to the observed width W_{21} to derive the corrected H I line width W_c.

seen in Figure 2*b*, the peak SNR of the spectra is high, on average 15.7. For comparison, the H I spectra included in Mathewson & Ford (1996) have a mean SNR, defined similarly, of 10.1. The minimum required SNR for TF applications depends on the shape of the H I profile, but a goal of SNR > 7 has been set by these observations where possible. The calculation of ϵ_W includes consideration of the SNR.

Figure 3 investigates the characteristics of the width measurements themselves. The two top panels show the variation of W_{21} with SNR (Fig. 3*a*) and estimated error on the width (Fig. 3*b*). Figure 3*c* displays the histogram of the corrections, $W_{21} - W_c$, applied to the observed width W_{21} to derive the corrected H I line width W_c. These distributions reflect the overall SFI sample: (1) there are almost no galaxies with small velocity widths $V < 100$ km s^{-1}; most widths are in the range $200 < W_{21} < 400$ km s^{-1}; and (2) while the highest SNR indeed occur for the smaller W_{21} galaxies, there is no systematic trend in SNR with W_{21}. Typical corrections to convert the observed W_{21} to W_c are on the order of 10–15 km s^{-1}, but in rare instances can exceed 20 km s^{-1}. It should be noted that the final error on the *turbulence and inclination-corrected* width will also incorporate a term for uncertainty in the viewing angle and in the turbulence correction.

6. RESULTS FOR DATA FROM LITERATURE

Adoption of a standard H I width definition that best measures the flat part of the rotation curve is particularly critical when the TF relation is applied to samples of mixed optical and radio spectral measurements. For the minority (215 of 1727) of galaxies included in our optical imaging sample (Haynes et al. 1999b), 21 cm line data are not available digitally. However, good quality H I line widths are available in the literature for 72 objects. Some of these include observations made by R. G. and M. P. H. primarily for the purposes of obtaining redshifts and measures of H I content. For those, the adopted width is the average of that measured at 50% of the mean flux and 20% of the peak flux. These two measures are typically similar (Bicay & Giovanelli 1986) and robust. However, widths measured by either of these prescriptions tend to overestimate that asymptotic circular velocity by ~ 20 km s^{-1}, and a measure closer to 50% of the peak is more appropriate (G98). Hence, it is necessary to be able to convert widths measured using other, but standard, algorithms to a scale common to W_{21}.

During our reprocessing procedure, we recorded velocity widths obtained using four different commonly used methods, in addition to W_{21}, namely widths measured at: (1) 50% of the mean flux, (2) 50% of the overall peak flux, (3) 20% of the peak flux on each horn separately, and (4) 50% of the peak flux on each horn separately. An overall database of some 3000 galaxies has been used to derive regression relations that relate one method to another. The coefficients of these regression relations are given in Table 2.

In those cases where the velocity width was derived from data in the literature, we have converted those parameters via the derived regression relations to comparable measurements of W_{21}. We emphasize that the use of regression relations degrades the treatment since in the absence of access to the digital data, the profile shape cannot be considered. Where available, we attempt to correct for resolution effects, but most often SNRs are not quoted in the literature. Where a rms noise figure is available, we estimate that the profile peak is the same on each horn and equal to $1.5 \int S\,dV/W_{21}$ and divide that by the rms to get a value of SNR. The factor 1.5 is obtained from examination of the actual SNRs, fluxes and widths in the digital archive. For other profiles, we assume SNR = 10. Where such information is not directly available, we have estimated the instrumental parameters from our knowledge of the spectrometers at the observatories used and typical observational setups.

In Table 3, we present the corrected H I line widths for 67 galaxies for which we have converted published values of observed width to an equivalent measure of W_{21} and then estimated a correction for instrumental broadening and noise. Columns (1)–(7) are identical to those in Table 1. Column (8) gives the corrected velocity width W_c. The source of the published H I width used to compute W_c is given in the last column.

Because the necessary observational parameters are not always available and no comparable estimate of the width error can be made, it is not possible to estimate the error on W_c for the data taken from the literature as precisely as for those available in the digital archive. However, we estimate that the typical error ϵ_W for the objects in Table 3 is about 10 km s^{-1}, somewhat larger than for the galaxies in Table 1 (see Fig. 1*f*).

7. SUMMARY

Together with results presented in Giovanelli (1997a) and Haynes et al. (1997), systematic H I widths are now available for 1515 galaxies with optical photometric properties presented in Haynes et al. (1999b). Additional H I observations conducted as part of the same observing program but for galaxies not included in the optical imaging survey will be

TABLE 3

PROPERTIES OF GALAXIES DERIVED FROM DATA IN LITERATURE

Number (1)	Other (2)	α(1950) (3)	δ(1950) (4)	$a \times b$ (5)	T (6)	$V_\odot$ (7)	W_c (8)	Reference (9)
39		00 02 59.0	+53 21 15	1.3 × 0.6	5	9523	476.1	1
400279.....	N151	00 31 30.1	−09 58 56	5.0 × 2.5	4	3748	431.3	2
369.....	N173	00 34 38.4	+01 40 03	4.0 × 3.5	4	4367	264.5	3
528.....	N278	00 49 14.8	+47 16 43	2.8 × 2.8	4	640	120.8	4
1537	M+804013	02 00 24.1	+48 12 58	1.4 × 0.2	5	7432	428.7	1
1983	N949	02 27 45.1	+36 54 53	3.6 × 2.3	5	612	186.0	5
2193	N1058	02 40 23.2	+37 07 48	3.8 × 3.7	5	520	15.4	2
2247	N1090	02 44 00.0	−00 27 20	4.3 × 2.1	5	2765	306.1	2
2510	N1171	03 00 40.0	+43 12 16	3.2 × 1.4	5	2747	255.6	2
2659	540−094	03 15 36.3	+40 24 53	1.3 × 0.5	4	6158	289.5	1
3120		04 36 48.0	+40 10 00	1.1 × 0.7	5	5676	229.1	1
3439	N2146a	06 15 54.2	+78 33 18	3.5 × 1.3	5	1495	209.9	2
3504	285−003	06 35 38.5	+60 07 43	2.9 × 2.5	5	2106	196.5	2
180631.....	U4345B	08 17 26.0	+21 15 53	0.5 × 0.4	5	6922	140.2	6
4345	N2562	08 17 28.6	+21 17 27	1.3 × 1.0	0	5074	620.5	6
4646	I512	08 50 57.0	+85 41 46	3.6 × 2.7	5	1614	113.3	2
190187.....	181−010	09 15 33.7	+32 29 00	0.7 × 0.3	3	8042	325.1	7
4952	N2814	09 17 09.2	+64 27 50	1.3 × 0.2	3	1589	375.9	4
26699	N3054	09 52 12.0	−25 27 57	3.6 × 2.3	4	2427	367.0	8
26706	I2522	09 52 58.0	−32 54 00	4.5 × 3.6	5	3018	289.5	2
27402	437 G 30	10 36 55.0	−30 02 17	4.4 × 0.8	5	3759	401.2	8
27462	N3347b	10 39 43.0	−36 40 24	4.2 × 1.0	5	3184	339.9	9
27475	N3347	10 40 29.0	−36 05 43	4.5 × 2.6	5	3001	407.7	8
27705	N3533	11 04 45.0	−36 54 05	4.5 × 1.0	5	3100	397.4	1
6453	N3684	11 24 34.3	+17 18 20	3.5 × 2.4	5	1171	200.2	10
210512.....	097−023	11 34 11.8	+20 16 59	0.2 × 0.2	−2	6630	245.7	11
510112.....	M−330003	11 35 27.0	−16 57 06	2.9 × 0.8	5	6546	518.0	1
210623.....	097−063	11 39 39.7	+20 19 28	0.4 × 0.3	3	6102	129.4	4
210637.....	097−073	11 40 18.6	+20 14 28	0.7 × 0.7	6	7290	262.6	12
210717.....	097−113	11 42 11.1	+20 02 07	0.6 × 0.2	−2	8293	504.0	11
210718.....	097−114	11 42 11.5	+20 03 02	0.5 × 0.3	1	8450	304.3	4
6718	N3860	11 42 13.2	+20 04 18	1.2 × 0.6	3	5595	448.2	13
6733	N3850	11 42 55.9	+56 09 48	2.2 × 1.0	5	1166	149.4	2
28167	504 G 25	11 51 18.0	−27 04 18	2.5 × 1.8	5	1637	109.1	9
28171	N3956	11 51 27.7	−20 17 17	3.6 × 1.2	5	1660	283.3	2
28319	I2995	12 03 12.5	−27 39 42	2.9 × 1.0	5	1851	211.6	2
7111	N4116	12 05 02.7	+02 58 15	3.8 × 2.5	5	1310	199.1	2
28350	573 G 2	12 05 06.0	−17 47 42	1.8 × 1.1	5	5790	176.1	4
7116	N4123	12 05 37.5	+03 09 30	5.0 × 4.0	4	1339	175.2	2
7371	N4268	12 17 13.9	+05 33 41	1.3 × 0.5	−2	2374	258.4	11
7418	N4302	12 19 10.2	+14 52 36	5.1 × 0.9	5	1145	345.2	3
28485	506 G 4	12 19 13.0	−23 53 30	2.6 × 1.3	4	4022	459.0	1
28661	N4575	12 35 08.0	−40 15 41	2.7 × 1.6	5	2973	250.1	8
520104.....	M−132035	12 37 40.7	−09 01 27	1.6 × 1.2	4	6360	243.3	4
520107.....	N4602	12 38 02.2	−04 51 27	4.6 × 2.0	5	2559	383.5	2
28708	N4603	12 38 12.0	−40 42 06	4.5 × 3.5	5	2562	455.9	2
28820	322 G 85	12 45 17.0	−40 19 17	1.7 × 0.4	5	3764	179.4	4
28923	323 G 25	12 49 52.0	−38 45 24	2.7 × 1.6	5	4221	353.3	8
221378.....	160−082	12 57 52.4	+27 39 31	0.5 × 0.4	3	11015	129.2	12
29264	UA 327	13 05 03.0	−22 35 24	4.2 × 0.7	5	2616	215.9	2
29274	575 G 61	13 05 34.0	−20 44 05	2.8 × 0.2	5	1643	117.5	8
29351	UA 334	13 10 09.0	−32 25 24	3.9 × 0.8	5	2382	194.2	2
29361	576 G 11	13 10 24.0	−19 42 48	3.9 × 0.6	5	2756	279.3	8
29371	N5022	13 10 49.4	−19 16 56	3.1 × 0.5	5	2991	306.7	8
29486	576 G 32	13 17 09.0	−22 01 00	3.1 × 2.2	5	1627	131.9	1
29627	444 G 33	13 23 15.0	−31 52 12	2.1 × 0.5	5	2423	172.2	9
8465	N5169	13 26 02.7	+46 55 48	2.1 × 0.7	5	2482	297.4	2
30139	383 G 91	13 47 35.0	−37 02 30	3.2 × 0.4	5	1079	124.2	9
8867	N5452	13 54 26.8	+78 27 56	2.3 × 1.8	5	2066	153.8	2
30766	512 G 12	14 37 17.0	−25 33 00	3.7 × 0.4	4	1839	201.7	4
251405.....	108−033	15 56 46.6	+15 04 11	0.7 × 0.3	1	12711	535.1	13
260081.....		16 02 04.8	+17 34 33	0.6 × 0.2	4	10804	392.3	4
260082.....	108−095	16 02 06.6	+16 50 14	0.8 × 0.3	3	9284	402.9	13
260114.....		16 02 32.1	+17 29 00	0.6 × 0.3	0	12320	307.8	4
10177	N6045	16 02 53.0	+17 53 34	1.1 × 0.2	3	10049	648.9	13

TABLE 3—*Continued*

Number (1)	Other (2)	α(1950) (3)	δ(1950) (4)	$a \times b$ (5)	T (6)	$V_\odot$ (7)	W_c (8)	Reference (9)
10192	I1182	16 03 21.9	+17 56 11	1.6 × 0.5	−6	10091	528.2	13
10195	108−136	16 03 38.0	+18 21 17	1.2 × 0.4	3	10721	540.6	13
10389		16 24 53.2	+39 14 14	1.1 × 0.4	3	6348	464.0	4
590033.....		19 43 10.2	−06 25 47	2.0 × 0.9	5	10178	526.3	1
610149.....	N7171	21 58 20.2	−13 30 37	3.2 × 2.1	4	2719	341.4	8
11946	545−004	22 09 37.3	+46 03 43	1.1 × 0.8	5	5536	333.0	4
12221	369−002	22 50 24.0	+82 36 40	2.5 × 0.8	5	2057	235.3	2

NOTE.—Units of right ascension are hours, minutes, and seconds, and units of declination are degrees, arcminutes, and arcseconds.

REFERENCES.—(1) Theureau et al. 1998; (2) Fisher & Tully 1981; (3) These observations but digital spectrum lost; (4) Richter & Huchtmeier 1989; (5) Haynes & Giovanelli 1984; (6) Eder et al. 1991; (7) Mould et al. 1995; (8) Mathewson & Ford 1996; (9) Fouqué et al. 1990; (10) Magri 1994; (11) Gavazzi et al. 1996; (12) Gavazzi 1989; (13) Giovanelli & Haynes 1985.

presented in Haynes, Giovanelli, & Chamaraux (1999a). The H I widths presented here are used for our analysis of the local peculiar velocity field via the TF relation (Giovanelli et al. 1997d, 1998b, 1998c; Borgani et al. 1997; da Costa et al. 1996, 1998; Freudling et al. 1999).

Observations at the 100 m telescope were partially supported by NSF grant AST 89-16985 to M. P. H. This work has been partially supported by NSF grants AST 90-14850, AST 90-23450, AST 92-18038, and AST 95-28860 to M. P. H., AST 91-15459, AST 94-20505, and AST 96-17069 to R. G., AST 95-53020 to J. J. S., and AST 93-47714 to G. W. Also, R. G. and M. H. thank the Observatoire de Nançay for hospitality during several visits there. H. G. Corwin kindly provided a digital copy of the *Southern Galaxy Catalog*. This research has made use of the NASA/IPAC Extragalactic Database (NED), which is operated by the Jet Propulsion Laboratory, Caltech, under contract with the National Aeronautics and Space Administration. We thank the expert technical staffs at the various observatories for their assistance and support throughout the many observing runs that contributed to this project.

REFERENCES

Aaronson, M., Huchra, J., & Mould, J. 1980, ApJ, 237, 655
Aaronson, M., & Mould, J. 1986, ApJ, 303, 1
Bicay, M. D., & Giovanelli, R. 1986, AJ, 91, 705
Borgani, S., da Costa, L. N., Freudling, W., Giovanelli, R., Haynes, M. P., Salzer, J. J., & Wegner, G. 1997, ApJ, 482, 121
Bottinelli, L., Gouguenheim, L., Paturel, G., & Teerikorpi, P. 1986, A&A, 166, 393
Bridle, A., Davis, M. M., Fomalont, E., & Lequeux, J. 1972, AJ, 77, 405
Corbelli, E., & Schneider, S. E. 1997, ApJ, 479, 244
Corwin, H. G., de Vaucouleurs, A., & de Vaucouleurs, G. H. 1985, Southern Galaxy Catalogue, Univ. Texas Monogr. Astron., 4, 1 (digital version)
da Costa, L. N., Freudling, W., Wegner, G., Giovanelli, R., Haynes, M. P., & Salzer, J. J. 1996, ApJ, 468, L5
da Costa, L. N., Nusser, A. Freudling, W., Giovanelli, R., Haynes, M. P., Salzer, J. J., & Wegner, G. 1998, MNRAS, 299, 425
de Vaucouleurs, G., de Vaucouleurs, A., Corwin, H. G., Buta, R. J., Paturel, G., & Fouqué, P. 1991, Third Reference Catalogue of Bright Galaxies (New York: Springer) (RC3)
Eder, J., Giovanelli, R., & Haynes, M. P. 1991, AJ, 102, 572
Federspiel, M., Sandage, A., & Tammann, G. A. 1994, ApJ, 430, 29
Fisher, J. R., & Tully, R. B. 1981, ApJS, 47, 139
Fouqué, P. 1982, Ph.D. thesis, Meudon
Fouqué, P., Bottinelli, L., Durand, N., Gouguenheim, L., & Paturel, G. 1990, A&AS, 86, 473
Freudling, W. F., da Costa, L. N., Wegner, G., Giovanelli, R., Haynes, M. P., & Salzer, J. J. 1995, AJ, 110, 920
Freudling, W., et al. 1999, ApJ, submitted
Fukugita, M., Okamura, S., & Yasuda, N. 1993, ApJ, 412, L13
Gavazzi, G. 1978, ApJ, 346, 59
Gavazzi, G., Pierini, D., & Boselli, A. 1996, A&A, 312, 397
Giovanelli, R., Avera, E., & Karachentsev, I. 1997a, AJ, 114, 1220
Giovanelli, R., Dale, D., Haynes, M. P., & Hardy, E. 1998a, AJ, submitted (G98)
Giovanelli, R., & Haynes, M. P. 1985, ApJ, 292, 404
———. 1989, AJ, 97, 633
Giovanelli, R., Haynes, M. P., da Costa, L. N., Freudling, W., Salzer, J. J., & Wegner, G. 1997b, ApJ, 477, L1
Giovanelli, R., Haynes, M. P., Herter, R., Vogt, N., da Costa, L. N., Freudling, W., Salzer, J. J., & Wegner, G. 1997c, AJ, 113, 22
———. 1997d, AJ, 113, 53
Giovanelli, R., Haynes, M. P., Salzer, J. J., Wegner, G., da Costa, L. N., & Freudling, W. 1998b, ApJ, 505, 91
———. 1998c, AJ, in press
———. 1994, AJ, 107, 2036
———. 1995, AJ, 110, 1059
Giovanelli, R, Haynes, M. P., Wegner, G., da Costa, L. N., Freudling, W., & Salzer, J. J. 1996, ApJ, 464, L99
Haynes, M. P., & Giovanelli, R. 1984, AJ, 89, 758
———. 1991, ApJS, 77, 331
Haynes, M. P., Giovanelli, R., & Chamaraux, P. 1999a, in preparation
Haynes, M. P., Giovanelli, R., Herter, T., Vogt, N. P., Freudling, W., Maia, M. A., Salzer, J. J., & Wegner, G. 1997, AJ, 113, 1197
Haynes, M. P., Giovanelli, R., Salzer, J. J., Wegner, G., Freudling, W., & da Costa L. N. 1999b, AJ, in press
Haynes, M. P., Hogg, D. E., Maddalena, R. J., Roberts, M. S., & van Zee, L. 1998, AJ, 115, 62
Lauberts, A. 1982, ESO-Uppsala Survey of the ESO(B) Atlas (Munich: ESO) (ESO)
Magri, C. 1994, AJ, 108, 896
Mathewson, D. S., & Ford, V. L. 1996, ApJS, 107, 97
Mould, J. R., Akeson, R. L., Bothun, G. D., Han, M., Huchra, J. P., Roth, J., & Schommer, R. A. 1993, ApJ, 409, 14
Mould, J. R., et al. 1991, ApJ, 383, 467
Mould, J., Martin, S., Bothun, G., Huchra, J., Schommer, B. 1995, ApJS, 96, 1
Nilson, P. 1973, Uppsala General Catalogue of Galaxies, Acta Univ. Uppsala Ser. V: A, Vol. 1, Uppsala (UGC)
Ott, M., Witzel, A., Quirrenbach, A., Krichbaum, T. P., Standke, K. J., Schalinski, C. I., & Hummel, C. A. 1994, A&A, 284, 331
Pierce, M. J., & Tully, R. B. 1988, ApJ, 330, 579
Richter, O.-G., & Huchtmeier, W. K. 1989, A General Catalog of H I Observations of Galaxies: The Reference Catalog (New York: Springer)
Schneider, S. E., Helou, G., Salpeter, E. E., & Terzian, Y. 1986, AJ, 92, 742
Teerikorpi, P. 1993, A&A, 280, 369
Theureau, G., Bottinelli, L., Coudreau-Durand, N., Gouguenheim, L., Hallet, N. Loulergue, M., Paturel, G., & Teerikorpi, P. 1998, A&A, 130, 333
van Zee, L., Maddalena, R., Haynes, M. P., Hogg, D. E., & Roberts, M. S. 1997, AJ, 113, 1638
Vorontsov-Velyaminov, B. A., & Arhipova, V. P. 1968, Morphological Catalog of Galaxies (Moscow: Moscow State Univ.) (MCG)
Wegner, G., Freudling, W., Haynes, M. P., Giovanelli, R., da Costa, L. N., & Salzer, J. J. 1999, in preparation
Williams, D. R. W. 1973, ApJS, 8, 505
Willick, J. 1989, ApJ, 351, L5
———. 1994, ApJS, 92, 1
Zwicky, F., Herzog, E., Karpowicz, M., Kowal, C., & Wild, P. 1961–1968, Catalogue of Galaxies and Clusters of Galaxies, Vols. 1–6 (Pasadena: Caltech) (CGCG)